PLK1 downregulation by RO3280 prevents cell proliferation, migration, and invasion via the Wnt/β-catenin pathway in prostate cancer

Yongxue Ding[1], Zhe Zhang[2], Min Ju[2]

[1]Department of Urology, Liaoyang City Central Hospital, Liaoyang, China
[2]Department of Urology, First Hospital of China Medical University, Shenyang, China

Submitted: 10 August 2021; **Accepted:** 22 August 2021
Online publication: 26 August 2021

Arch Med Sci
DOI: https://doi.org/10.5114/aoms/141508

Corresponding author:
Dr. Min Ju
Zhe Zhang
Department of Urology
First Hospital of China
Medical University
155 Nanjing North St
Heping District
Shenyang City 110001
Liaoning Province
China
E-mail: jumin_cmu@163.com,
zhangzhe@cmu1h.com

Abstract

Introduction: Higher expression levels of serine/threonine-protein kinase 1 (PLK1) are significantly associated with tumorigenesis and poor clinical prognoses. Consequently, PLK1 is considered a latent target in cancer treatment. We aimed to determine the cytotoxic effects of RO3280 on prostate cancer cells.

Material and methods: PLK1 expression was investigated using real-time PCR and western blotting in prostate cancer tissues and paired normal tissues. Real-time cell analysis, Cell Counting Kit-8 assays, and 5-ethynyl-2′-deoxyuridine cell proliferation assays were applied for the examination of cell proliferation ability. Wound healing assays and transwell assays were used to assess the migratory and invasive abilities of the prostate cancer cell lines with or without RO3280 treatment. Moreover, the target genes and pathways were detected by transcriptomics RNA sequencing in the cells cultured in RO3280 and through a series of bioinformatic analyses. Finally, the Wnt/β-catenin pathway was screened out and verified by western blotting.

Results: We observed the mRNA and protein overexpression of PLK1 in the prostate cancer cells and tissues. The inhibition of PLK1 by RO3280 significantly reduced the migratory, invasive, and proliferative properties of the RO3280-treated cancer cell lines compared with their controls. RO3280 mediated the inactivation of the Wnt/β-catenin pathway, and reduced the rates of cell proliferation, migration, and invasion in prostate cancer cells.

Conclusions: This study's findings are significant owing to the identification of the specific anticancer mechanism of RO3280, which may have therapeutic effects. This trial provides clarity on the feasibility of the use of RO3280 as a cancer therapeutic agent for prostate cancer.

Key words: prostate cancer, PLK1 RO3280, proliferation, migration, invasion.

Introduction

Prostate cancer is among the most pernicious tumors of the genitourinary system and is the second most commonly observed cause of cancer-related death among men in Western countries [1]. The diverse clinical behaviors of prostate cancer include a sloth-like characteristic with little or no clinical value, invasive metastasis, and lethality [2, 3]. Nevertheless, there are no critical clinical signals that are credible for use in the anticipation of the response to prostate cancer therapy, owing to

the disparate actions of prostate cancer. In consequence, it is meaningful to explore the etiopathogenesis of prostate cancer for the development of specific biomarkers and treatment.

Serine/threonine-protein kinase 1 (PLK1) is the most comprehensively investigated of the five subtypes of the polo-like family of serine/threonine kinases [4]. PLK1 is abnormally expressed in solid tumors and higher expression is associated with poor prognosis [5]. While the activity of PLK1 is downregulated or inhibited in a majority of cancer cell types *in vivo* and *in vitro*, it could guide cell cycle arrest and apoptosis. A large number of small molecule inhibitors for PLK1 have been identified so far, and the potential of PLK1 inhibitors in cancer treatment has been inspected proverbially [6–9]. Of these inhibitors, RO3280 has shown latent antiproliferative activity in several cancer cell lines, and exhibited stable antineoplastic activity in bladder cancer [10]. While PLK1 is among the targets of RO3280, the inhibitor has almost no action towards PLK2 and PLK3. RO3280 suppresses the rate of cell proliferation in leukemia in a dose-dependent pattern and brings about apoptosis [11].

In the carcinogenesis of tumors, the Wnt/β-catenin signaling pathway has a role in proliferation and apoptosis [12–14]. A previous study showed that the Wnt/β-catenin pathway is closely associated with tumor progression [15]. The translocation of the transcription factor β-catenin from the cytoplasm to the nucleus can have on effect on its target genes – MMP7 and c-Myc – which have significant roles in metastasis and disease progression [16, 17].

Previous studies have demonstrated that RO3280 can decrease the rates of cell proliferation, invasion and metastasis in diverse cancers; however, the definite mechanism through which it inhibits the degree of epithelial mesenchymal transition (EMT) and metastasis in prostate cancer remains poorly understood. Moreover, there is a lack of clarity on the possible role of the Wnt/β-catenin signaling pathway in the antitumor effect of RO3280 on prostate cancer cells. Therefore, in the present study, we sought to evaluate the antitumor effect of RO3280 on prostate cancer cells, as well as the role of the Wnt/β-catenin pathway in the promotion of tumor progression.

Material and methods

Patients and prostate cancer samples

A total of 60 prostate cancer tissues and paired adjacent normal tissues were acquired through biopsy or surgical resection from the Department of Urology in the First Hospital of China Medical University between January 2018 and August 2020. Tissues were stored at –80°C. The 60 enrolled prostate cancer patients were aged 53–71 years (average: 60.2 years). The inclusion criteria for enrollment were: 1) prostate cancer diagnosed before surgery, consistent with the biopsy pathological diagnosis; 2) absence of other pernicious diseases or a second primary tumor; 3) absence of chemotherapy or radiotherapy before surgery; and 4) provision of informed consent for the collection of specimens. All the experiments were approved by the Ethics Committee of the First Hospital of China Medical University.

Cell culture and transfection

Prostate cell lines were purchased from the company BNBIO (China). Cells were maintained in RPMI-1640 medium containing 10% fetal bovine serum (FBS, Invitrogen, MO, USA) in an incubator at 37°C with 5% CO_2.

Lentivirus carrying PLK1-wt was produced by the company Genechem (Shanghai, China), and the viruses were transduced into the prostate cancer cells. Cells with PLK1 overexpression were screened with puromycin (Invitrogen, NY, USA) and evaluated by western blotting.

Real-time quantitative polymerase chain reaction

We extracted total RNA using RNAiso Plus (TAKARA BIO INC., Shiga, Japan), and cDNA synthesis was performed with a cDNA Synthesis Kit (TAKARA Company Takara Bio, Shiga, Japan). Quantitative real-time polymerase chain reaction (PCR) assays were performed with SYBR Green, following the manufacturer's protocol (TAKARA Company, Shiga, Japan). The PLK1 primer sequences were 5′-CAAGAAGAATGAATACAGTA-3′ and 5′-GGATATAGCCAGAAGTAA-3′. The primers sequences of β-actin are 5′-CAAGCCGTAGGACCCAGTTT-3′ and 5′-CACAATGACGTGTTGCTGGG-3′. We normalized the levels of expression of PLK1 relative to β-actin, and $2^{-\Delta\Delta Ct}$ indicated the quantification of gene expression.

Western blot analysis

Cells were collected in phosphate-buffered saline and lysed in RIPA lysis buffer including proteinase inhibitors (KeyGEN BioTECH, Nanjing, China) following the manufacturer's protocols. Bicinchoninic acid assays (KeyGEN BioTECH, Nanjing, China) were performed for the examination of protein concentrations. A total of 50 µg of protein was transferred onto sodium dodecyl sulfate-polyacrylamide electrophoresis gels and then onto polyvinylidene difluoride membranes (Millipore, MA, USA). Tris/saline solution co'n-

taining 5% non-fat milk and 0.1% Tween-20 was used to block all the membranes for 1 h. The membranes were probed with specific primary antibody: mouse monoclonal anti-PLK1 antibody (ab17056, 1 : 2000, Abcam, Cambridge, MA), rabbit monoclonal anti-GAPDH antibody (ab181602, 1 : 5000, Abcam, Cambridge, MA), rabbit monoclonal anti-Wnt3a antibody (#2721, 1 : 2000, Cell Signaling Technology, USA), rabbit monoclonal anti-GSK-3β antibody (#12456, 1 : 2000, Cell Signaling Technology, USA), rabbit monoclonal anti-β-Catenin antibody (#8480, 1 : 2000, Cell Signaling Technology, USA), rabbit monoclonal anti-c-Myc antibody (#18583, 1 : 2000, Cell Signaling Technology, USA), and rabbit monoclonal anti-Cyclin D1 antibody (#55506, 1 : 2000, Cell Signaling Technology, USA). After massive washing, horseradish peroxidase-conjugated secondary antibodies (1 : 10,000; Cell Signaling Technology, USA) were applied for incubation with the membranes for 1 h at room temperature. The target protein bands were explored using an enhanced chemiluminescence kit (Thermo; Rockford, IL).

Real-time xCELLigence cell proliferation assay

The Real-Time xCELLigence system (ACEA Biosciences, San Diego, CA, USA) was used to observe the degree of cytotoxicity employing electronic sensor array technology. The cells were planted into an E-plate 16 (each well with 100 µl of medium) at a thickness of 2 × 10^4 cells/well. When the cells entered the log phase, RO3280 treatment (0–100 ng/ml) was performed in three independent experiments (n = 3). The concentration of dimethylsulfoxide (DMSO) in every group did not exceed 5% (v/v). Cells were treated with RO3280 for 24 h at 37°C in 5% CO_2. The cell index and half maximal inhibitory concentration (IC_{50}) values were obtained based on the cell-electrode impedance value, which is directly related to cell survival capability and quantity.

Cell Counting Kit-8 assays

Cell Counting Kit (CCK)-8 was used for the evaluation of cell viability. In short, 5,000 cells per well were planted into 96-well plates for 24 h. After treatment with the IC_{50} of RO3280 for about 48 h, 10 µl of CCK-8 solution was added to each well. The cells were maintained for an extra 2 h at 37°C. The absorbance at 450 nm was detected with a microplate reader (Bio Rad, CA, USA) in the plate. Cell proliferation ability was measured as the ratio of the absorbance at 48 h to that at 0 h and was determined by three independent experiments.

5-ethynyl-2′-deoxyuridine proliferation assay

We utilized 5-ethynyl-2′-deoxyuridine (EdU) proliferation assays for the evaluation of cell proliferation capacity as per the protocol. After the RO3280 culture cycle, the prostate cancer cells were treated for 2 h using EdU (RiboBio, Nanjing, China). Following Apollo staining and 4′,6-diamidino-2-phenylindole staining (Thermo Fisher Scientific), fluorescence microscopy (Olympus, Tokyo, Japan) was applied for the assessment of EdU-positive cells.

Wound healing assay

After treatment with RO3280 for 48 h, a cell monolayer was scraped with a 200-µl pipette tip. The medium was refreshed with a serum-free medium. At 0 h and 24 h, every scratch wound was observed using a microscope at the same position. All experiments were performed in triplicate.

Transwell assay

The prostate cancer cells were seeded into the upper chamber of Corning transwell inserts (Sigma-Aldrich, MO, USA) enclosed with or without Matrigel for the invasion or migration experiments, respectively. Absolute medium was added to the lower chamber. After incubation for 24 h, the cells showing infiltration to the bottom were dyed with crystal violet solution. The cells showing invasion or migration through the membrane were examined in five stochastically chosen fields by a microscope (Olympus, Tokyo, Japan) at a magnification of 100×.

RNA extraction, library preparation and RNA sequencing

After total RNA extraction, mRNA was replenished using Oligo(dT) beads. Then rRNA was removed and prokaryotic mRNA enriched by the Ribo-Zero Magnetic Kit (Epicentre) was made. The concentrated mRNA was shattered into short pieces using a fragmentation buffer and reverse transcribed into cDNA with random primers. Second-strand cDNA composition was performed using DNA polymerase I, RNase H, dNTP, and buffer. The cDNA fragments were also refined with the QIAquick PCR extraction kit, and underwent end repair, poly(A) addition, and ligation to Illumina sequencing adapters. The ligation products were chosen by agarose gel electrophoresis, amplified using PCR, and sequenced using the Illumina HiSeq 2500 by Gene Denovo Biotechnology Co. (Guangzhou, China).

Differentially expressed gene analysis

The edgeR package (http://www.rproject.org/) was applied for the identification of differentially

expressed genes (DEGs). The genes were identified with a fold change ≥ 2 and a false discovery rate < 0.05 in contrast with the values for meaningful DEGs. The DEGs were then subjected to gene ontology (GO) function and KEGG pathway enrichment analyses.

GO and KEGG pathway analyses of DEGs

GO analysis is a method used for the definition of genes and gene outcomes considering their characteristic biological functions, based on high-throughput genome or transcriptome data. KEGG is a set of databases with information on genomes and biological pathways. The Database for Annotation Visualization and Integrated Discovery (DAVID: http://david.ncifcrf.gov) (version 6.8) comprising information on the biological functions of genes and analytical tools was applied for the classification of the GO and KEGG pathways of the identified co-expressed DEGs. The false discovery rate threshold was set at $p < 0.05$.

Ethics approval and consent to participate

The study protocols were approved by the Ethics Committee of the First Hospital of China Medical University (permit number: 2018-190-2), China.

No animals were used for studies that are the basis of this research.

Statistical analysis

GraphPad Prism 6.0 statistical software (GraphPad Software, Inc., CA, USA) and SPSS 20.0 (IBM Corp., NY, USA) were utilized for data analyses. The DAVID tool was employed in the pathway enrichment analysis. A two-tailed paired Student's *t*-test was used for the analysis of between-group comparisons. One-way analysis of variance and a Bonferroni post hoc test were applied for the assessment of differences across multiple groups. For categorical variables, we used the χ^2 or Fisher's exact test. $P < 0.05$ was indicative of statistical significance.

Results

PLK1 is overexpressed in clinical prostate cancer samples

To evaluate the level of PLK1 expression in prostate cancer, we first used quantitative real-time PCR analysis for examination of the clinical prostate cancer tissues. PLK1 showed significantly higher expression levels in the prostate cancer tissues than the adjacent normal prostate tissues (Figure 1 A). To further confirm the expression level of PLK1 in the prostate cancer samples, western blotting was performed in the prostate cancer samples obtained from patients who underwent surgery. The results demonstrated that the level of PLK1 was reasonably upregulated in the prostate cancer tissues compared with that in the normal prostate tissues (Figures 1 B, C). We also measured the level of PLK1 mRNA and protein expression in the prostate cancer cell lines – LNCaP, 22RV1, DU145, and PC3 – and the normal prostate epithelial cell line – RWPE-1. All four prostate cancer cell lines exhibited higher PLK1 mRNA and protein expression levels than the RWPE-1 cell line (Figures 1 D–F). These findings indicate that PLK1 overexpression was present at the mRNA and protein levels in the prostate cancer cells and tissues.

RO3280 inhibits cell proliferation of prostate cancer

A previously published study reported that RO3280 exerts antitumor effects, facilitated predominantly by DNA damage, cell cycle arrest, and apoptosis in breast cancer cells [2]. In our previous study too, we found that RO3280 repressed bladder carcinoma growth through G2/M arrest and mitotic arrest [6]. The *in vitro* proliferative activity doses of RO3280 in the 22RV1 and PC3 cell lines were measured using the xCELLigence real-time cell analysis instrument. After 48 h of incubation with RO3280, the IC_{50} value was found to be 29.1 nM for the 22RV1 cell line and 32.3 nM for the PC3 cell line (Figures 2 A, B). The effect of RO3280 on prostate cancer cell proliferation was also appraised utilizing CCK-8 proliferation assays. We found that the degree of cell proliferation was remarkably decreased with RO3280 treatment over 48 h (IC_{50} value, Figures 2 C, D). Meanwhile, the EdU proliferation assay showed that the number of prostate cancer cells in the RO3280 group was obviously lower than that in the DMSO group (Figures 2 E, F), indicating that RO3280 exerted an obvious inhibitory effect on these prostate cancer cell lines.

RO3280 attenuated the invasive and migratory ability of 22RV1 and PC3 cells

As cell migration and invasion are characteristic features of prostate cancer metastasis, we investigated the antimetastatic potential of RO3280 using wound healing and transwell assays. In the wound healing assay, the level of cell migration was examined every 12 h for 2 days, and images were visualized using a microscope at 10× magnification. The wound healing rates of the 22RV1 and PC3 cells in the RO3280 group were obviously lower than those in the DMSO group at every measurement point (Figures 3 A, B). Moreover, transwell assays that were performed for the investigation of cell migration and invasion showed that the invasive and migratory abilities of 22RV1 and PC3 were obviously lower in the RO3280

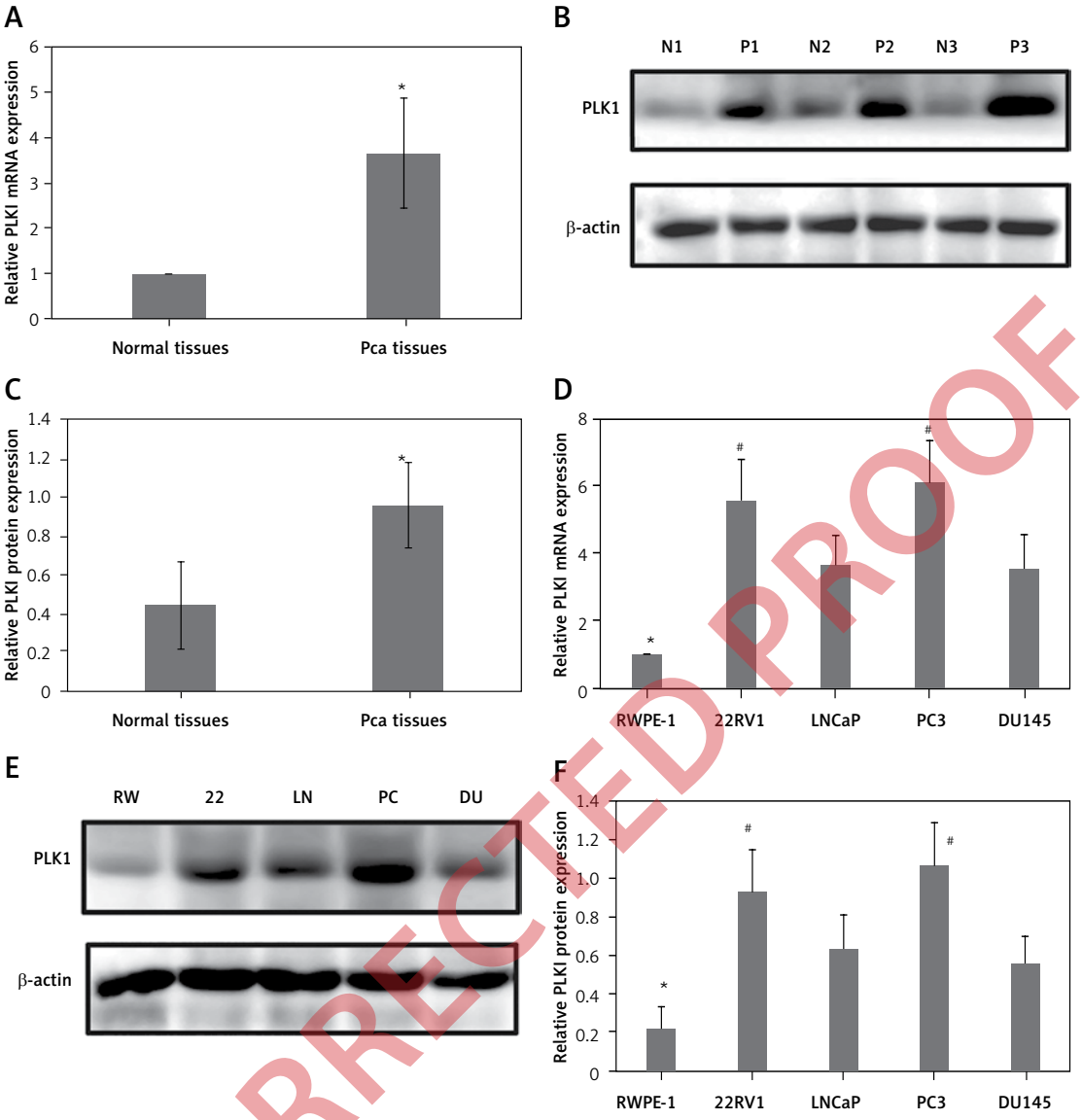

Figure 1. mRNA and protein expression of PLK1 in prostate cancer tissues and prostate cancer cell lines. **A**, **B** – The mRNA ($p < 0.0001$) and protein expression levels of PLK1 in prostate cancer tissues ($n = 60$) and the adjacent non-tumor tissues ($n = 60$) were measured by RT-qPCR and western blot analysis. **C** – The ratio of the optical density of PLK1 and β-actin of the same sample using western blot analysis was calculated and expressed graphically ($p < 0.0001$). **D**, **E** – The mRNA and protein expression levels of PLK1 in the normal prostate epithelial cell line RWPE-1 and prostate cancer cell lines LNCaP, 22RV1, DU145, PC3 were measured by RT-qPCR (*RWPE-1 group vs. other cell groups, $p < 0.0001$; #22RV1 vs. LNCap, $p = 0.0009$; #PC3 vs. DU145, $p < 0.0001$;) and western blot analysis. **F** – The ratio of the optical density of PLK1 and β-actin of the same cells using western blot analysis was calculated and expressed graphically (*RWPE-1 group vs. other cell groups, $p < 0.0001$; #22RV1 vs. LNCap, $p = 0.0038$; #PC3 vs. DU145, $p < 0.0001$)

N1, N2, N3 – normal prostate tissues, P1, P2, P3 – prostate cancer tissues, RW – RWPE-1, 22 – 22RV1, LN – LNCaP, PC – PC3, DU – DU145. PLK1 – serine/threonine-protein kinase 1, RT-qPCR – real-time quantitative polymerase chain reaction.

group than in the DMSO group (Figures 3 C–F). These data demonstrate that RO3280 may have the potential to impair the invasive and migratory capacity of prostate cancer cells.

Identification of RO3280-related factors using transcriptomic analysis

While the real-time analysis of cell proliferation demonstrated that 48-hour treatment with RO3280 (IC_{50} value) was sufficient for the remarkable inflection of the 22RV1 and PC3 cell proliferation and regulation of proliferation and metastasis-related transcriptional signals, we confirmed the presence of genome-wide transcriptomic variations via RNAseq in PC3 on RO3280 treatment. The results demonstrated that the number of differentially expressed genes was 313 in the RO3280 group (Figures 4 A). Using the DAVID tool, we performed GO and KEGG pathway enrichment

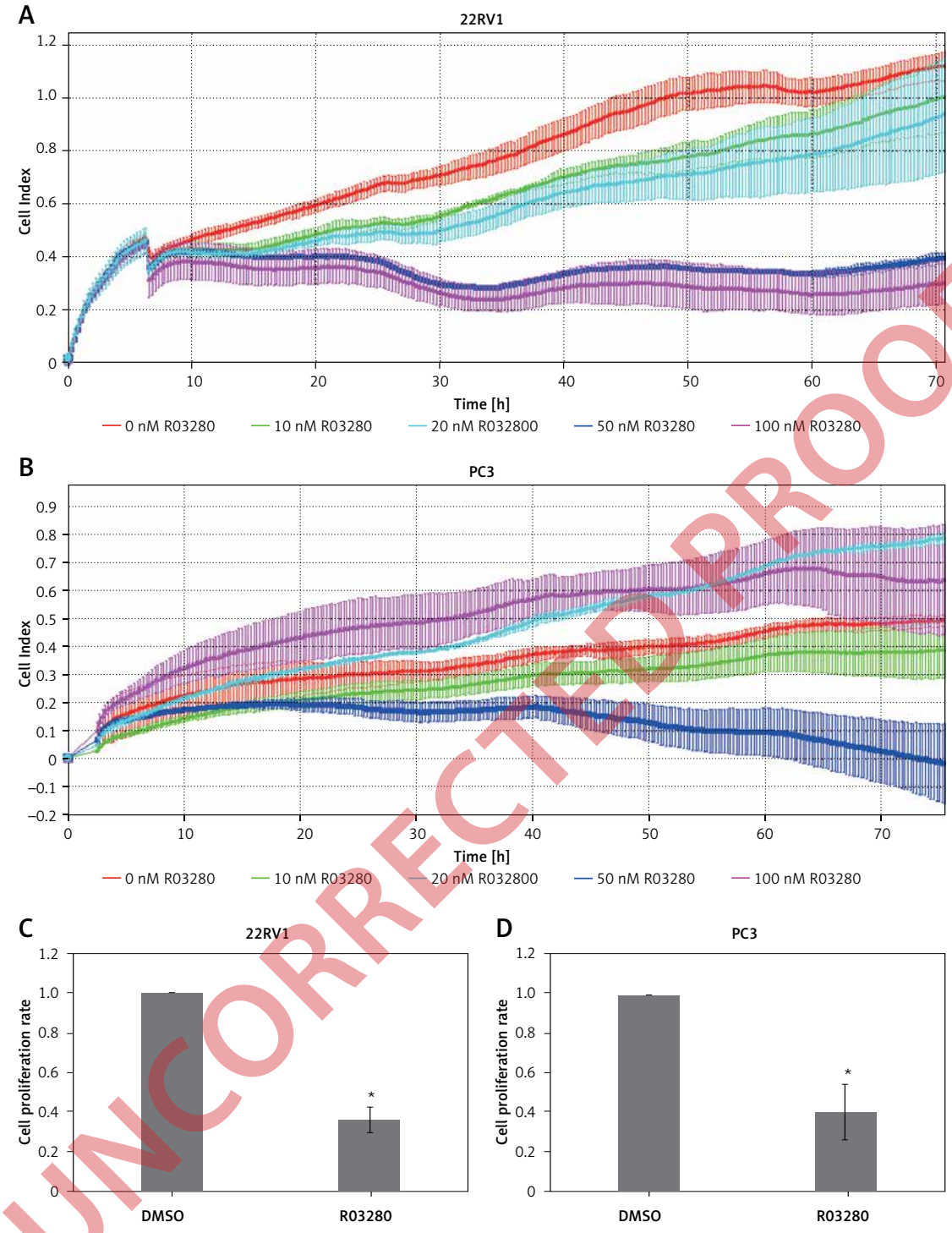

Figure 2. RO3280 inhibits cell proliferation in prostate cancer. **A**, **B** – Cell proliferation rates of the 22RV1 and PC3 cell lines cultured with 0, 10, 20, 50 and 100 nM RO3280 were measured using the xCELLigence real-time cell analysis instrument. **C**, **D** – Viabilities of the 22RV1 and PC3 cells cultured with the IC_{50} of RO3280 for 48 h were assessed by CCK-8 assay

**p < 0.05. IC_{50} – half maximal inhibitory concentration, CCK – Cell Counting Kit, EdU – 5-ethynyl-2'-deoxyuridine.*

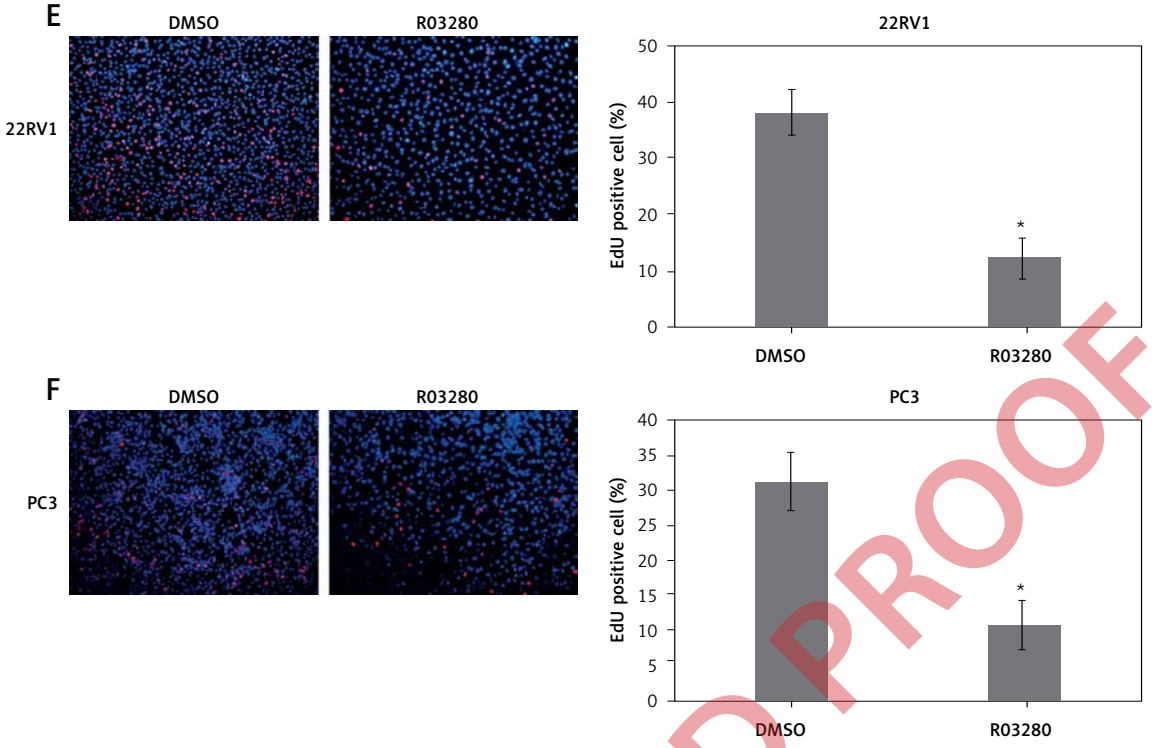

Figure 2. Cont. **E**, **F** – Cell proliferation abilities of the 22RV1 and PC3 cells cultured with the IC_{50} of RO3280 for 48 h were assessed by EdU proliferation assay

**p < 0.05. IC_{50} – half maximal inhibitory concentration, CCK – Cell Counting Kit, EdU – 5-ethynyl-2′-deoxyuridine.*

analyses of the identified DEGs, and found that the DEGs were predominantly involved in DNA replication, cell division, and cell migration (Figures 4 B–E). The Wnt/β-catenin pathway was significantly enriched, and the q-value of this pathway was close to zero.

RO3280 shows anticancer potential through suppression of the Wnt/β-catenin signaling pathway

The outcomes of the RNAseq-based approach indicate that RO3280 exerted cytotoxic effects on the biological behaviors of the prostate cancer cells through regulation of the Wnt/β-catenin signaling pathway. Then, we evaluated the expression levels of the Wnt/β-catenin related genes using western blotting. RO3280 hindered the protein expression levels of Wnt target genes, including Wnt3, GSK3β, β-catenin, c-Myc and cyclin D1 in the 22RV1 and PC3 cells, suggesting inactivation of the Wnt signaling pathway (Figures 5 A–D). Interestingly, in the prostate cancer cells treated with RO3280, the simultaneous overexpression of PLK1 (specific RO3280-targeted gene) resulted in an increase in the protein expression levels. This provides evidence that one possible mechanism by which RO3280 triggers inactivation of the Wnt pathway is through PLK1 mediation.

Discussion

In the present study, we found that RO3280 mediated the inactivation of Wnt/β-catenin signaling in prostate cancer cells, as well as reducing the rates of cell proliferation, migration and invasion. Mounting evidence indicates that PLK1 has therapeutic potential in several cancers, including prostate cancer [18–20]. In our previous study, we observed high PLK1 expression levels in prostate cancer tissues and prostate cancer cell lines, similar to the findings of previous studies. Treatment with PLK1 inhibitors was found to lead to marked improvements in the therapeutic susceptibility of paclitaxel-resistant prostate cancer in one study [21], while another group identified the novel non-canonical role of PLK1 as a critical regulator of EMT and cell movement in normal prostate tissues and prostate cancer [22]. Taken together, the aforementioned results as well as our findings demonstrate that PLK1 might participate in the development of prostate cancer and play an important role in the cell proliferation, invasion and metastasis of prostate cancer.

In recent decades, various biologically active derivatives obtained from medicinal plants have attracted extensive attention in cancer therapy owing to their promising efficacy and the presentation of fewer side effects. RO3280 has been recognized as having antitumor potential in sever-

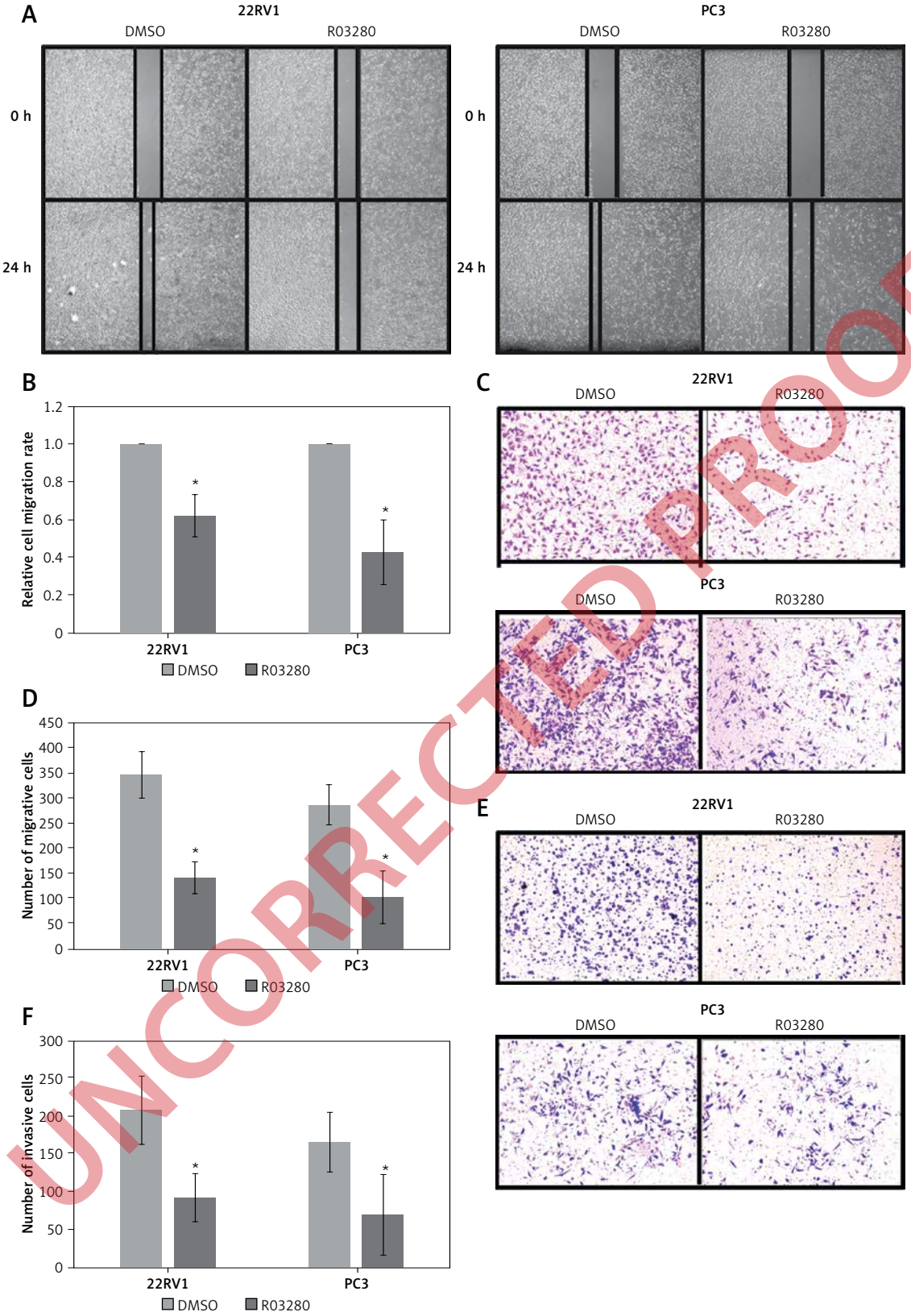

Figure 3. RO3280 attenuated the invasion and migration ability of 22RV1 and PC3 cells. **A**, **B** – Cell migration ability was examined by a wound healing assay in the 22RV1 and PC3 cells with or without RO3280. **C**, **D** – Cell migration ability was examined by a transwell assay without Matrigel in the 22RV1 and PC3 cells with or without RO3280. **E**, **F** – Cell invasion ability was examined by a transwell assay with Matrigel in the 22RV1 and PC3 cells with or without RO3280

**p < 0.05.*

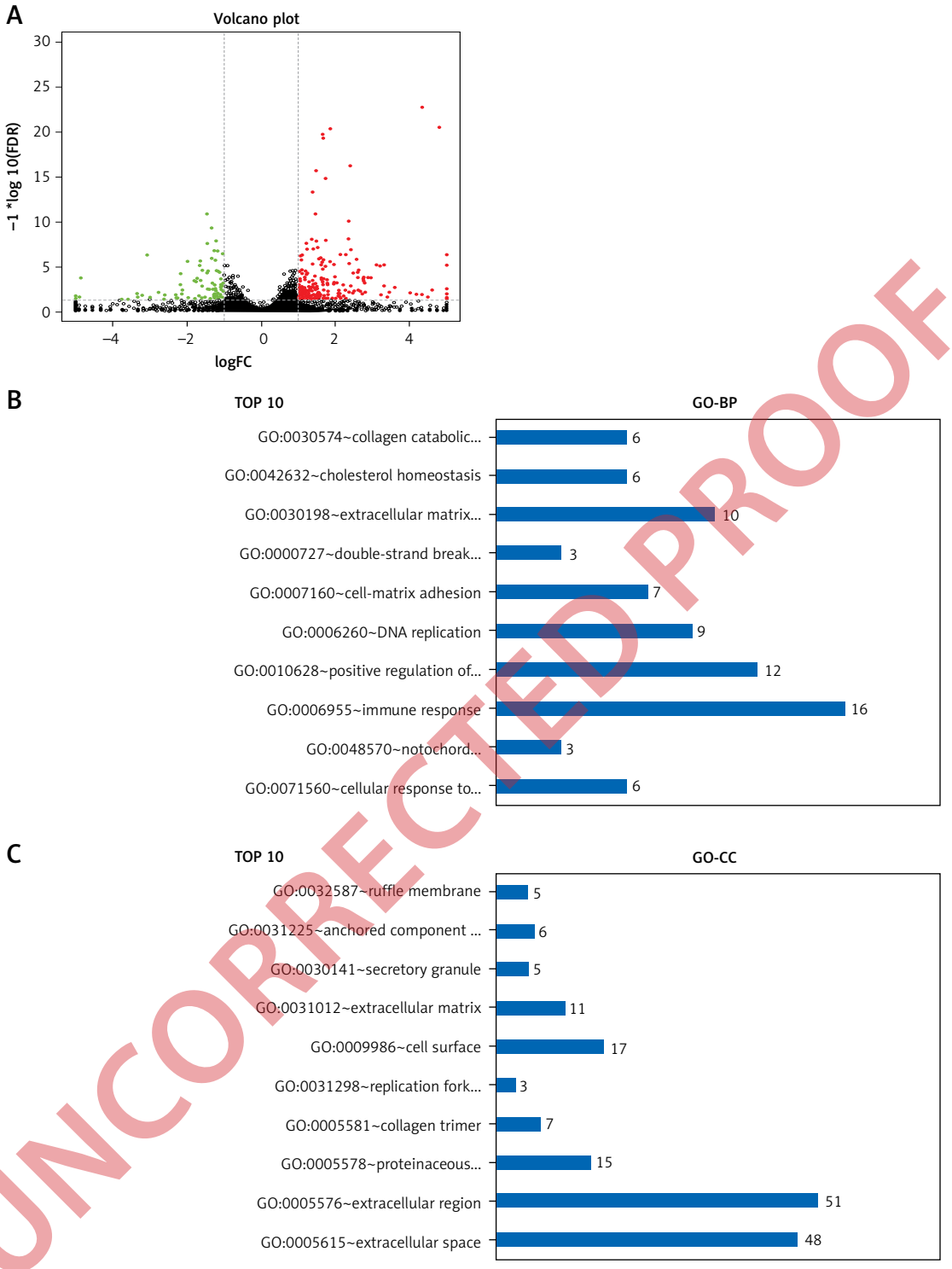

Figure 4. Identification of RO3280-related factors by transcriptomic analysis. **A** – Volcano plot indicated mRNA up-regulation and downregulation in the cells with and without RO3280 treatment, respectively. **B**–**D** – Top 10 terms in the GO enrichment analysis pertaining to biological process (**B**), cellular components (**C**)

GO – gene ontology, KEGG – Kyoto Encyclopedia of Genes and Genomes.

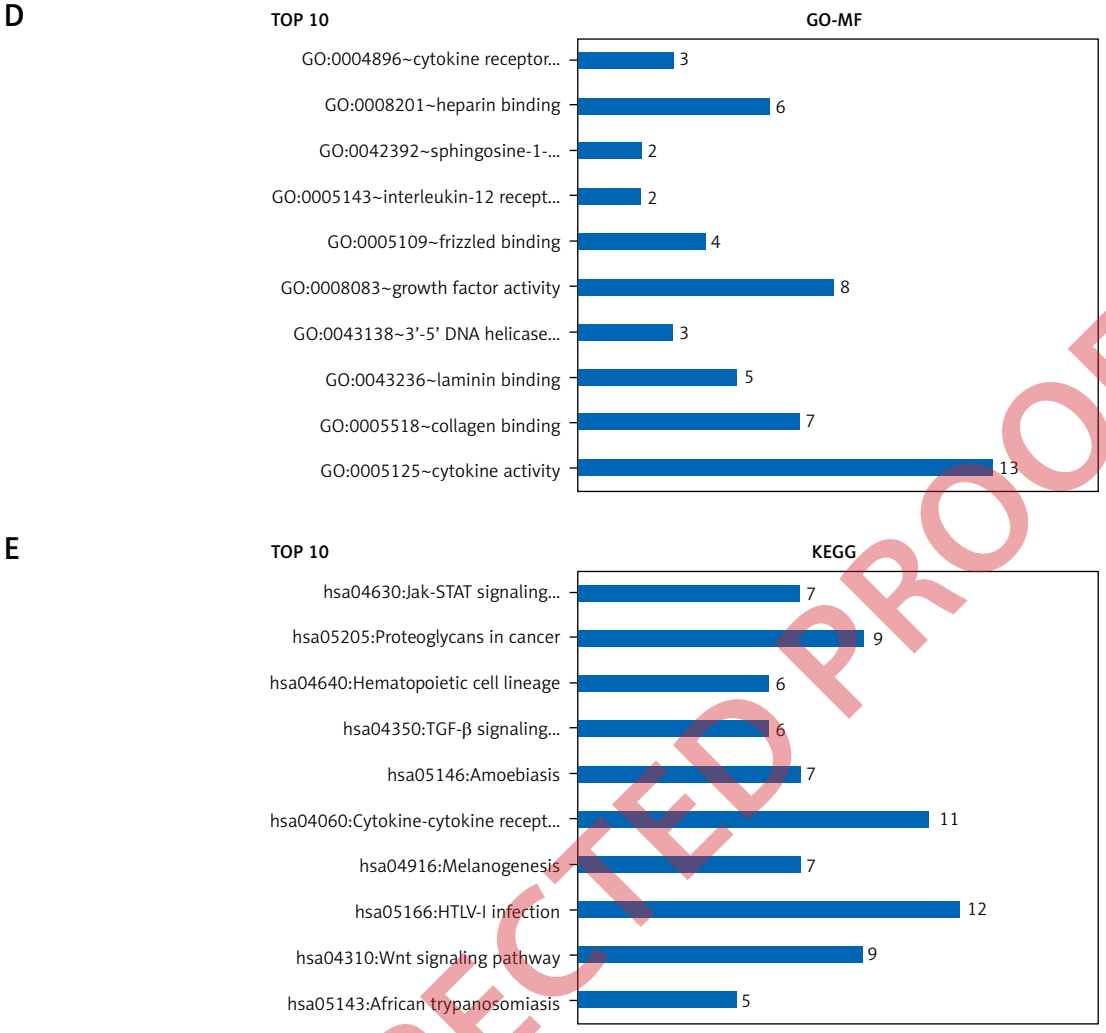

Figure 4. Cont. **B**–**D** – Top 10 terms in the GO enrichment analysis pertaining to biological process (**B**), cellular components (**C**) and molecular function (**D**). **E** – Top 10 terms in the KEGG pathway analysis

GO – gene ontology, KEGG – Kyoto Encyclopedia of Genes and Genomes.

al types of cancer, including breast cancer, acute myeloid leukemia and bladder cancer [6, 10, 23]. However, the antitumor effect of RO3280 on prostate cancer cells remains poorly understood. In the current study, the inhibition of PLK1 by RO3280 led to significant reductions in the strength of the migratory, invasive, and proliferative properties of RO3280-treated cancer cell lines compared with the values in the respective DMSO controls. These findings indicate that RO3280 treatment may provide a new approach for prostate cancer management.

Our transcriptome analysis results indicate that the most highly enriched GO terms and KEGG pathways of the DEGs included the response to RO3280. The number of DEGs associated with RO3280 treatment was 313. Furthermore, the DEGs were chiefly involved in DNA replication, cell division, and cell migration. Among them, Wnt/β-catenin signaling was significantly enriched, and the q-value of this pathway was close to zero.

Apart from the involvement of the aforementioned mechanism in RO3280-induced antitumor activity, the abnormal activation of Wnt/β-catenin signaling is implicated in both the pathogenesis of prostate cancer and development of resistance to anticancer therapies [24], suggesting that the targeted inhibition of individual components in this manner may have potential in cancer therapy. The role of the Wnt/β-catenin pathway is critical in cellular biological processes such as cell growth and differentiation [25, 26]. In the process of exerting its effects on the Wnt/β-catenin pathway, the level of β-catenin is augmented in the cytoplasm and the factor is transferred to the nucleus. The transcription of target genes principally containing cyclin D1 and c-Myc was found to be activated by β-catenin [27]. Abnormal activation of the Wnt/β-catenin pathway has been repeatedly observed in a large number of cancers [28–30]. Therefore, we examined whether RO3280 inhibits the activation of this pathway in 22RV1 and PC3

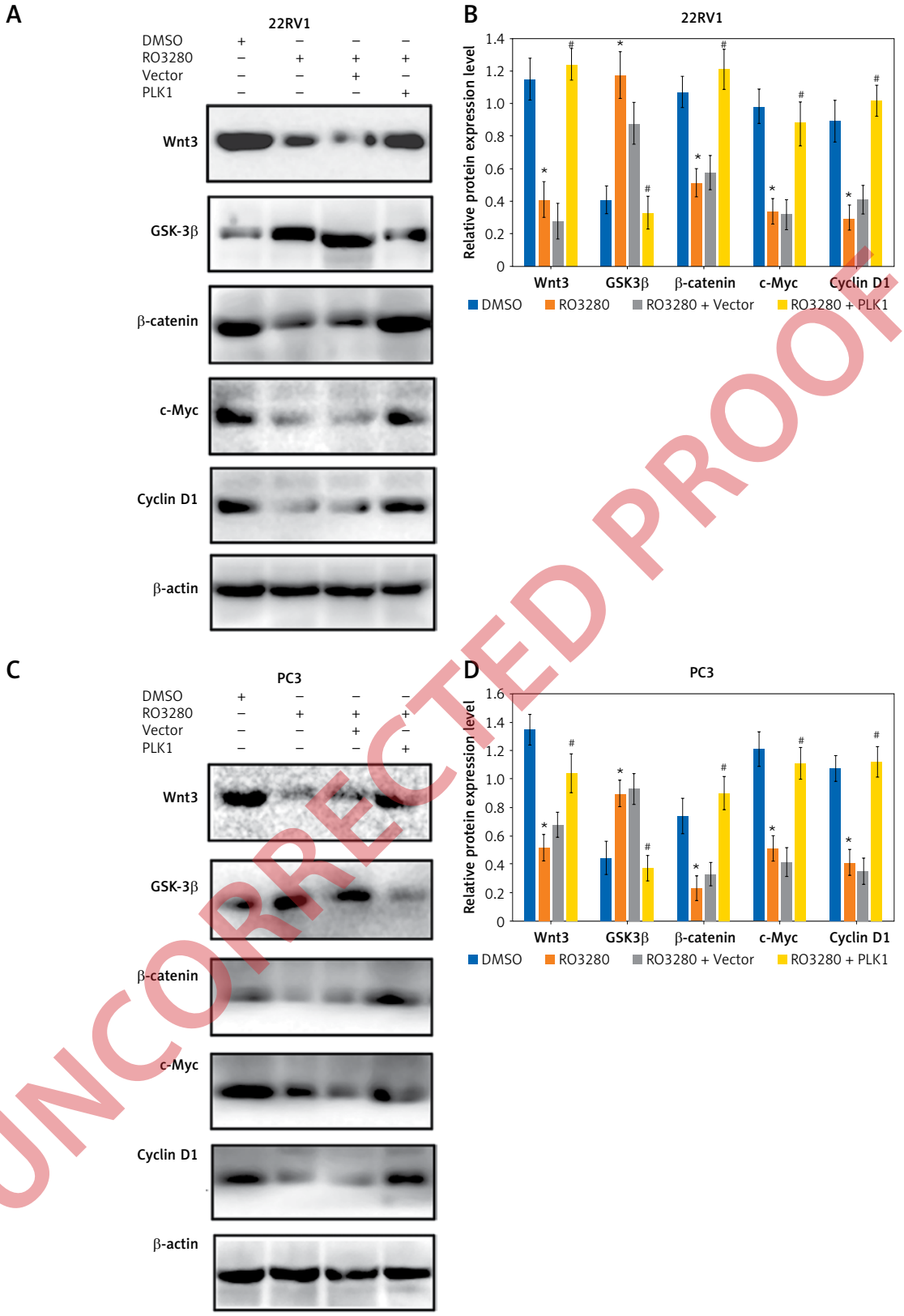

Figure 5. RO3280 exerts anticancer effects through suppression of the Wnt/β-catenin signaling pathway. Western blot analysis was used to detect the protein expression levels of Wnt3, GSK3β, β-catenin, c-Myc and cyclin D1 in the 22RV1 cells (**A**) and PC3 cells (**C**). **B**, **D** – Column graphs were used to present the statistical results of multiple **A** and **C** experiments

*Vector – pCDNA3.1, PLK1 – pCDNA3.1-PLK1-wild type plasmid, *DMSO vs. RO3280, #RO3280 + Vector vs. RO3280 + PLK1. *,#p < 0.05. PLK1 – serine/threonine-protein kinase 1, DMSO – dimethyl sulfoxide.*

cancer cells. RO3280 reduced the expression levels of Wnt3, GSK3β, β-catenin, c-Myc and cyclin D1 of the Wnt/β-catenin pathway, suggesting that the effects of RO3280 on the tumorigenesis of prostate cancer may be partly attributed to inactivation of the Wnt/β-catenin pathway.

In conclusion, the findings of this study may be of significance owing to the identification of the specific anticancer mechanism of RO3280, and may have therapeutic potential. To the best of our knowledge, our study is the first to demonstrate that RO3280 mediates the inactivation of Wnt/β-catenin signaling in prostate cancer cells, as well as reducing the rates of cell proliferation, migration and invasion. The results of this trial provide clarity on the feasibility of the use of RO3280 in cancer therapeutics for prostate cancer. However, the anticancer mechanism of RO3280 should be further investigated in animal models of prostate cancer.

Acknowledgments

This work was supported by Provincial Natural Science Foundation of Liaoning (Grant No. 2019-MS-378). The funding agency did not participate in the design of the study, in collection, analysis and interpretation of data, or in writing the manuscript.

Conflict of interest

The authors declare no conflict of interest.

References

1. de Almeida D, Fong L, Rettig MB, Autio KA. Immune Checkpoint blockade for prostate cancer: niche role or next breakthrough. Am Soc Clin Oncol Educ Book 2020; 40: 1-18.
2. Sklinda K, Mruk B, Walecki J. Active surveillance of prostate cancer using multiparametric magnetic resonance imaging: a review of the current role and future perspectives. Med Sci Monit 2020; 26: e920252.
3. Dragan J, Kania J, Salagierski M. Active surveillance in prostate cancer management: where do we stand now. Arch Med Sci 2021; 17: 805-11.
4. Goroshchuk O, Kolosenko I, Vidarsdottir L, Azimi A, Palm-Apergi C. Polo-like kinases and acute leukemia. Oncogene 2019; 38: 1-16.
5. Ng WTW, Shin JS, Roberts TL, Wang B, Lee CS. Molecular interactions of polo-like kinase 1 in human cancers. J Clin Pathol 2016; 69: 557-62.
6. Ergul M, Bakar-Ates F. RO3280: a novel PLK1 inhibitor, suppressed the proliferation of MCF-7 breast cancer cells through the induction of cell cycle arrest at G2/M point. Anticancer Agents Med Chem 2019; 19: 1846-54.
7. Kannan S, Aitken M, Herbrich SM, et al. Antileukemia effects of notch-mediated inhibition of oncogenic PLK1 in B-cell acute lymphoblastic leukemia. Mol Cancer Ther 2019; 18: 1615-27.
8. Li Z, Yang C, Li X, et al. The dual role of BI 2536, a small-molecule inhibitor that targets PLK1, in induction of apoptosis and attenuation of autophagy in neuroblastoma cells. J Cancer 2020; 11: 3274-87.
9. Van den Bossche J, Deben C, De Pauw I, et al. In vitro study of the Polo-like kinase 1 inhibitor volasertib in non-small-cell lung cancer reveals a role for the tumor suppressor p53. Mol Oncol 2019; 13: 1196-213.
10. Zhang Z, Zhang G, Kong C. Targeted inhibition of Polo-like kinase 1 by a novel small-molecule inhibitor induces mitotic catastrophe and apoptosis in human bladder cancer cells. J Cell Mol Med 2017; 21: 758-67.
11. Tao YF, Li ZH, Du WW, et al. Inhibiting PLK1 induces autophagy of acute myeloid leukemia cells via mammalian target of rapamycin pathway dephosphorylation. Oncol Rep 2017; 37: 1419-29.
12. Li L, Duan Q, Zeng Z, et al. UHRF2 promotes intestinal tumorigenesis through stabilization of TCF4 mediated Wnt/β-catenin signaling. Int J Cancer 2020; 147: 2239-52.
13. Li Y, Ma Y, Zhang T, Feng C, Liu Y. High-mobility group box 3 (HMGB3) silencing inhibits non-small cell lung cancer development through regulating Wnt/β-catenin pathway. Biol Chem 2020; 401: 1191-8.
14. Que LM, Yang XR, Zhang YC, Zhong H. MicroRNA-9501 inhibits breast cancer proliferation and metastasis through regulating Wnt/β-catenin pathway. Eur Rev Med Pharmacol Sci 2020; 24: 4337-47.
15. Shao S, Fang H, Duan L, et al. Lysyl hydroxylase 3 increases collagen deposition and promotes pulmonary fibrosis by activating TGFβ1/Smad3 and Wnt/β-catenin pathways. Arch Med Sci 2020; 16: 436-45.
16. Liu Y, Chen H, Dong P, et al. KIF23 activated Wnt/β-catenin signaling pathway through direct interaction with Amer1 in gastric cancer. Aging 2020; 12: 8372-96.
17. Ma B, Ma J, Yang Y, He X, Pan X, Wang Z, Qian Y. Effects of miR-330-3p on invasion, migration and EMT of gastric cancer cells by targeting PRRX1-mediated Wnt/β-catenin signaling pathway. Onco Targets Ther 2020; 13: 3411-23.
18. Dalvi PS, Macheleidt IF, Lim SY, et al. LSD1 inhibition attenuates tumor growth by disrupting PLK1 mitotic pathway. Mol Cancer Res 2019; 17: 1326-37.
19. Song R, Hou G, Yang J, et al. Effects of PLK1 on proliferation, invasion and metastasis of gastric cancer cells through epithelial-mesenchymal transition. Oncol Lett 2018; 16: 5739-44.
20. Yan W, Yu H, Li W, et al. Plk1 promotes the migration of human lung adenocarcinoma epithelial cells via STAT3 signaling. Oncol Lett 2018; 16: 6801-7.
21. Shin SB, Woo SU, Yim H. Cotargeting Plk1 and androgen receptor enhances the therapeutic sensitivity of paclitaxel-resistant prostate cancer. Ther Adv Med Oncol 2019; 11: 1758835919846375.
22. Wu J, Ivanov AI, Fisher PB, Fu Z. Polo-like kinase 1 induces epithelial-to-mesenchymal transition and promotes epithelial cell motility by activating CRAF/ERK signaling. Elife 2016; 5: e10734.
23. Wang NN, Li ZH, Zhao H, et al. Molecular targeting of the oncoprotein PLK1 in pediatric acute myeloid leukemia: RO3280, a novel PLK1 inhibitor, induces apoptosis in leukemia cells. Int J Mol Sci 2015; 16: 1266-92.
24. Zhu M, Yu X, Zheng Z, Huang J, Yang X, Shi H. Capsaicin suppressed activity of prostate cancer stem cells by inhibition of Wnt/β-catenin pathway. Phytother Res 2020; 34: 817-24.
25. Martin-Orozco E, Sanchez-Fernandez A, Ortiz-Parra I, Ayala-San Nicolas M. WNT signaling in tumors: the way to evade drugs and immunity. Front Immunol 2019; 10: 2854.

26. Oichi T, Otsuru S, Usami Y, Enomoto-Iwamoto M, Iwamoto M. Wnt signaling in chondroprogenitors during long bone development and growth. Bone 2020; 137: 115368.
27. Li K, Zhang J, Tian Y, et al. The Wnt/β-catenin/VASP positive feedback loop drives cell proliferation and migration in breast cancer. Oncogene 2020; 39: 2258-74.
28. Yang C, Wang Y, Yang W, Gao Y, Zhao B, Yang X. MiR-509-5p improves the proliferative and invasive abilities of papillary thyroid carcinoma cells by inhibiting SFRP1. Arch Med Sci 2019; 15: 968-78.
29. Suryawanshi A, Hussein MS, Prasad PD, Manicassamy S. Wnt signaling cascade in dendritic cells and regulation of anti-tumor immunity. Front Immunol 2020; 11: 122.
30. Chiarini F, Paganelli F, Martelli AM, Evangelisti C. The role played by Wnt/β-catenin signaling pathway in acute lymphoblastic leukemia. Int J Mol Sci 2020; 21: 1098.